

## Tumor Localization and *in vivo* Antitumor Activity of the Immunoconjugate Composed of Anti-human Colon Cancer Monoclonal Antibody and Mitomycin C-Dextran Conjugate

Akinori Noguchi,<sup>1,3</sup> Toshio Takahashi,<sup>1</sup> Toshiharu Yamaguchi,<sup>1</sup> Kazuya Kitamura,<sup>1</sup> Yoshinobu Takakura,<sup>2</sup> Mitsuru Hashida<sup>2</sup> and Hitoshi Sezaki<sup>2</sup>

<sup>1</sup>Department of Surgery, Kyoto Prefectural University of Medicine, Kawaramachi, Hirokoji, Kamigyo-ku, Kyoto 602 and <sup>2</sup>Department of Basic Pharmaceutics, Faculty of Pharmaceutical Sciences, Kyoto University, Yoshida-shimoadachicho, Sakyo-ku, Kyoto 606

The tissue distribution and *in vivo* antitumor activity of a novel monoclonal antibody-mitomycin C conjugate (A7-MMCD) composed of anti-human MAb A7 and MMC-dextran conjugate were investigated using tumor-bearing mice. A7-MMCD was prepared via an anionic dextran intermediate for the purpose of keeping the non-specific uptake by the reticuloendothelial system to a minimum. <sup>111</sup>In-labeled A7-MMCD showed about a 5-times-greater accumulation in SW1116 (targeted tumor) than in S180 (non-targeted tumor) 48 h after injection, and produced a tumor-to-blood ratio which was 3 times higher in SW1116-bearing mice than in S180-bearing mice 96 h after injection. Accumulations in the liver, spleen, and kidney were also observed to some extent. Pharmacokinetic analysis revealed that A7-MMCD had nearly the same properties in the body as MMCD<sub>an</sub> (MMCD with an anionic charge), i.e., those of a negatively charged macromolecule. Both A7-MMCD and MMCD<sub>an</sub> had relatively similar tissue uptake rate indices for the liver and spleen. The tumor uptake rate index for SW1116 was about 2.5 times greater than that for S180, and the total amount of <sup>111</sup>In-A7-MMCD accumulated in SW1116 was calculated to be approximately 5 times greater than the amount in S180. These results indicated that A7-MMCD could achieve site-specific targeting in the body. Furthermore, in the therapeutic experiment using SW1116 implanted subcutaneously, A7-MMCD suppressed tumor growth significantly, compared to free MMC and MMCD<sub>an</sub>. These results suggest that in designing an monoclonal antibody-drug conjugate via an intermediary, the physicochemical properties of intermediate macromolecules must also be taken into consideration to obtain a high degree of efficacy *in vivo*.

Key words: Monoclonal antibody A7 — Mitomycin C-dextran conjugate — Monoclonal antibody-drug conjugate — Tissue distribution

In recent years, monoclonal antibodies (MAbs)<sup>4</sup> that recognize tumor-associated cell surface antigens have been widely utilized as tumor-specific carriers for cytotoxic agents such as toxins, radioisotopes, and anti-cancer drugs.<sup>1,2</sup> In the case of MAb-drug conjugates, intermediate carriers such as polysaccharides, proteins, and synthetic polymers are currently being used to bind a sufficient amount of drug without impairing antibody binding activities.<sup>3-5</sup> However, although there have been many reports on successful preparations and the superior antitumor activities of such immunoconjugates, few evaluations have been done on their biodistribution. In fact, in these cases, intermediate macromolecules may affect the *in vivo* behavior of the parent conjugates, so it

is important to determine whether such conjugates achieve site-specific targeting *in vivo* as does the MAb alone before assessing their *in vivo* antitumor activity.

We have developed a novel immunoconjugate (A7-MMCD) composed of anti-human colon cancer MAb A7 and the polymeric prodrug of mitomycin C (MMC), mitomycin C-dextran conjugate with an anionic charge (MMCD<sub>an</sub>).<sup>6</sup> We designed this immunoconjugate for greater tumor localization, since our previous work had revealed that MMCD<sub>an</sub> is suitable for conjugation with MAb because of its long circulating life after intravenous administration owing to its physicochemical properties.<sup>7</sup>

In this study, an investigation of the tissue distribution of A7-MMCD was performed, including a pharmacokinetic analysis. *In vivo* antitumor activities were also evaluated in the preliminary experiment.

### MATERIALS AND METHODS

**Chemicals** MMC was kindly supplied by Kyowa Hakko Kogyo Co. (Tokyo). Dextran with an average molecular weight of about 70,000 (T-70) was purchased from

<sup>4</sup> Abbreviations: MAb, monoclonal antibody; MMC, mitomycin C; MMCD, MMC-dextran conjugate; MMCD<sub>an</sub>, MMCD with an anionic charge; MMCD<sub>cat</sub>, MMCD with a cationic charge; PBS, phosphate-buffered saline; DTPA, diethylenetriaminepentaacetic acid; AUC, the area under the plasma concentration-time curve; S180, sarcoma 180; SPDP, N-succinimidyl 3-(2-pyridyldithio)propionate.

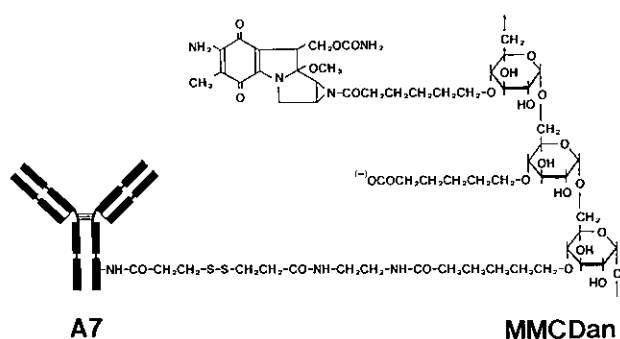


Fig. 1. Chemical structure of A7-MMCD.

Pharmacia (Uppsala). Radioactive indium chloride [<sup>111</sup>In]Cl<sub>3</sub> was supplied by Nihon Mediphysics, Takarazuka, Osaka. All other chemicals were reagent grade products obtained commercially.

**Monoclonal antibody** The MAb A7 used in this study was an IgG1, secreted from a hybridoma produced after the fusion of mouse myeloma cells and spleen cells from BALB/c mice immunized with a human colon cancer cell line.<sup>8)</sup> The MAb was purified from murine ascitic fluid by affinity chromatography on immobilized Protein A. Isolated MAb A7 was dialyzed against PBS and stocked in a freezer (-70°C).

**Preparation of MMCD<sub>an</sub> and A7-MMCD** MMCD<sub>an</sub> and A7-MMCD were synthesized using a dextran (T-70) as reported previously.<sup>6,9)</sup> The chemical structure of A7-MMCD is shown in Fig. 1. The antibody binding activity and drug activity of A7-MMCD were almost completely preserved after the conjugation procedure. The molar binding ratio was estimated to be 1:1.2:40 (IgG:dextran:MMC). In addition, A7-MMCD, as well as MMCD<sub>an</sub>, was found to be inert by itself but released active MMC with a half-life of about 30 h under physiological conditions (pH 7.4, 37°C).

**Indium-111 labeling** The A7-MMCD was labeled with <sup>111</sup>In using a bifunctional chelating agent, DTPA anhydride, according to the method of Hnatowich *et al.*<sup>10)</sup> with several modifications. To the A7-MMCD solution (5 mg/ml in 0.1 M NaHCO<sub>3</sub>) was added 1.5 mol of DTPA anhydride (Dojindo Laboratories, Kumamoto) dissolved in 10 μl of dry dimethyl sulfoxide (DMSO). The mixture was stirred for 30 min at room temperature and purified by gel filtration with Sephadex G-25 (Pharmacia) to separate the free DTPA. DTPA-coupled A7-MMCD solution (960 μl) was added to a mixture of 480 μl of <sup>111</sup>InCl<sub>3</sub> solution (2 mCi/ml in 0.01 N HCl) and 480 μl of 1 M sodium acetate buffer (pH 6.0). After a 30 min incubation at room temperature, unbound <sup>111</sup>In was removed by ultrafiltration and more than 60% of <sup>111</sup>In

was calculated to bind to A7-MMCD. The specific activity was 5–10 mCi/mg.

**Tumors and animals** Male ddY mice and BALB/c (*nu/nu*) female athymic mice were obtained from the Shizuoka Agricultural Co-operative Association for Laboratory Animals, Shizuoka. Sarcoma 180 (S180), which was used as the A7 reactive antigen-negative cell line, was maintained in ddY mice by weekly intraperitoneal (ip) transfer of 10<sup>5</sup> cells obtained from ascitic fluid. For the tissue distribution study, one-tenth of one milliliter of ascitic fluid was inoculated subcutaneously into ddY mice. The colon cancer cell line, SW1116, serving as the A7 reactive antigen-positive cell line, was grown in a monolayer culture in RPMI 1640 medium supplemented with 10% heat-inactivated fetal calf serum. SW1116 xenografts initiated from the *in vitro* tumor cell line were subsequently passed subcutaneously in nude mice and used for the biodistribution and therapeutic studies.

**Tissue distribution study procedure** Ten to fourteen days after tumor inoculation, when the tumor became measurable (about 5–10 mm in diameter), nude mice bearing SW1116 and ddY mice bearing S180 were injected with <sup>111</sup>In-labeled A7-MMCD into the tail vein at a dose of 50 μg of antibody in 0.2 ml of PBS. At 1, 24, 48, and 96 h after injection, blood was collected from the vena cava and the mice were killed. Organs, such as the heart, lung, liver, spleen, kidney, intestines, muscle, lymph nodes and tumor were excised, and weighed, and their radioactivities were measured in a gamma scintillation counter.

**Pharmacokinetic analysis** The level of the macromolecule in the plasma was analyzed using a two-compartment open pharmacokinetic model. The analysis was performed using the non-linear least-squares program MULTI.<sup>11)</sup> The plasma concentration was best described by the biexponential equation.

$$C_p(t) = Ae^{-\alpha t} + Be^{-\beta t}$$

where B=C<sub>0</sub> (the concentration at time 0)–A. This analysis yielded the half-life of the macromolecule in the α and β phases of clearance and the concentration constants A and B. The AUC was calculated from the obtained parameters. The AUC at infinite time is given by

$$AUC = A/\alpha + B/\beta$$

On the other hand, the tissue distribution of the macromolecule was evaluated using a tissue uptake rate index calculated in terms of clearance, as reported previously.<sup>7)</sup> The change in the tissue concentration of a macromolecule with time can be described as follows:

$$dT(t)/dt = Cl_{in} \times C(t) - K_{out} \times T(t) \quad (1)$$

where T(t) is the amount of macromolecule in 1 g of tissue, C(t) is the plasma concentration, Cl<sub>in</sub> is the tissue

uptake rate index (clearance) from the plasma to the tissue, and  $K_{out}$  is the efflux rate constant from the tissue. In the present study, efflux processes of the macromolecule, such as return to the plasma after breakdown in the tissue, should be almost negligible, since the radioactivity of the  $^{111}\text{In}$  would be retained for a long period in the tissue. Therefore, Eq. (1) integrates to

$$Cl_{in} = T(t_1)/C(t_1)dt = T(t_1)/AUC_{0-t_1} \quad (2)$$

According to Eq. (2), the tissue uptake rate index is calculated using the amount of the macromolecule in the tissue and the AUC. Values obtained 96 h after injection were used for the calculation of the tissue uptake rate of the macromolecule. Then, organ clearance ( $Cl_{org}$ ) can be expressed as follows:

$$Cl_{org} = Cl_{in} \times W \quad (3)$$

where  $W$  is the total weight of the organ. In addition, the total body clearance ( $Cl_{total}$ ) equals the sum of each organ clearance, and the following equation should hold.

$$Cl_{total} = \text{Dose}/\text{AUC} = Cl_{liver} + Cl_{kidney} + \dots + Cl_{tumor} \quad (4)$$

Furthermore, the total tumor accumulation at infinite time was calculated to compare the levels of tumor uptake for the various compounds used, according to the following equation, which assumes the tumor weight to be 1 g.

$$\text{Total tumor accumulation (\% of dose)} = Cl_{tumor} \times 1/Cl_{total} \times 100 \quad (5)$$

**Therapeutic experiment** The SW1116 xenograft initiated from an *in vitro* tumor cell line was subsequently passed subcutaneously in nude mice. Eleven days after tumor

inoculation, when the tumor became measurable, the mice were divided into an appropriate number of groups with each group consisting of four mice. The test compound in 0.2 ml of PBS was intravenously injected into the tumor-bearing mice (on day 11 and day 19). The tumor size was measured with a caliper at 2- or 3-day intervals, and the volume was calculated by using the equation  $V = (a \times b^2)/2$ , where  $a$  is the length (mm),  $b$  is the width (mm), and  $V$  is the volume ( $\text{mm}^3$ ) of the tumor. For a comparison among different groups, the mean relative tumor volume (RV) for each group was calculated from the formula  $RV = V_i/V_0$ , where  $V_i$  is the mean tumor volume at any given time and  $V_0$  is the mean initial tumor volume when the treatment began. Since each tumor's growth rate was variable, the ratio of RV of the treated group to RV of the control group (T/C) was calculated.

## RESULTS

**Tissue distribution** Tables I and II show the tissue distribution of radioactivity after iv injection of  $^{111}\text{In}$ -labeled A7-MMCD in ddY mice bearing S180 (non-target tumor) and nude mice bearing SW1116 (target tumor), respectively. Radioactivity concentrations in the heart, lung, intestines, and muscle were very low in both cases. In S180-bearing mice, marked accumulation of radioactivity was observed in the liver, spleen, and kidney, but the radioactivity concentration in the tumor was very low. On the other hand, although significant accumulations in the liver, spleen, and kidney were also observed in SW1116-bearing mice, a marked accumulation of radioactivity was noted in the tumor. In fact,  $^{111}\text{In}$ -A7-MMCD showed about a 5-times-greater accu-

Table I. Tissue Distribution of  $^{111}\text{In}$ -A7-MMCD after Intravenous Injection into Nude Mice Bearing SW1116 (N=3)

Organ	% injected dose/g or ml at time postinjection			
	1 h	24 h	48 h	96 h
Heart	1.89 ± 0.11 <sup>a)</sup>	1.75 ± 0.17	2.01 ± 0.36	1.03 ± 0.25
Lung	2.74 ± 0.26	3.11 ± 0.48	3.13 ± 0.87	1.83 ± 0.20
Liver	20.23 ± 0.34	30.67 ± 3.26	25.46 ± 4.41	15.89 ± 1.47
Spleen	8.56 ± 1.25	16.02 ± 2.02	20.62 ± 3.03	15.41 ± 1.30
Kidney	17.47 ± 1.53	15.99 ± 0.18	15.96 ± 2.68	9.11 ± 1.06
Intestines	0.62 ± 0.09	2.49 ± 0.12	2.00 ± 0.63	1.04 ± 0.08
Muscle	0.61 ± 0.11	0.52 ± 0.11	0.86 ± 0.18	0.64 ± 0.17
Lymph nodes	ND	12.97 ± 20.07	53.79 ± 48.48	11.92 ± 4.70
Tumor	3.60 ± 0.44	15.87 ± 4.71	19.70 ± 4.47	15.78 ± 4.62
Plasma	34.99 ± 3.58	5.70 ± 0.51	3.45 ± 0.32	1.11 ± 0.18
Body weight (g)	27.7 ± 2.70	29.0 ± 1.74	28.4 ± 0.30	

a) Mean ± SD.

Table II. Tissue Distribution of  $^{111}\text{In}$ -A7-MMCD after Intravenous Injection into ddY Mice Bearing S180 (N=4)

Organ	% injected dose/g or ml at time postinjection			
	1 h	24 h	48 h	96 h
Heart	$1.71 \pm 0.53^a)$	$0.97 \pm 0.18$	$1.34 \pm 0.20$	$0.60 \pm 0.13$
Lung	$1.46 \pm 0.45$	$1.23 \pm 0.19$	$1.23 \pm 0.14$	$0.84 \pm 0.25$
Liver	$13.96 \pm 1.35$	$20.41 \pm 1.51$	$13.69 \pm 0.50$	$8.65 \pm 1.73$
Spleen	$5.03 \pm 0.46$	$9.31 \pm 1.73$	$11.98 \pm 1.60$	$6.12 \pm 2.55$
Kidney	$14.40 \pm 1.56$	$23.26 \pm 3.26$	$14.40 \pm 1.60$	$8.71 \pm 1.29$
Intestines	$0.47 \pm 1.45$	$2.70 \pm 0.31$	$0.96 \pm 0.10$	$0.39 \pm 0.08$
Muscle	$0.59 \pm 0.11$	$0.41 \pm 0.15$	$0.67 \pm 0.12$	$0.45 \pm 0.13$
Lymph nodes	$8.28 \pm 8.96$	$15.67 \pm 9.22$	$20.54 \pm 16.41$	$10.21 \pm 7.70$
Tumor	$0.56 \pm 0.23$	$3.03 \pm 0.34$	$3.91 \pm 0.73$	$1.93 \pm 0.41$
Plasma	$19.29 \pm 2.02$	$2.36 \pm 0.69$	$1.52 \pm 0.24$	$0.38 \pm 0.13$
Urine (% of dose)			$2.08 \pm 1.09$	
Body weight (g)	$29.1 \pm 2.45$	$29.0 \pm 1.49$	$26.4 \pm 1.71$	

a) Mean  $\pm$  SD.

mulation in SW1116 than in S180, 48 h after injection ( $19.70 \pm 4.47\%$  dose/g in SW1116,  $3.91 \pm 0.73\%$  dose/g in S180). As for the tissue-to-blood ratio, A7-MMCD produced a tumor-to-blood ratio which was 3 times higher in SW1116-bearing mice than in S180-bearing mice, 96 h after injection (13.4 for SW1116, 4.8 for S180).

**Pharmacokinetic analysis** To evaluate quantitatively the tissue distribution observed in this study, tissue uptake rate indices were calculated in terms of clearance by dividing the tissue level by AUC. Table III summarizes the AUCs, total body clearances, tissue uptake indices for some representative organs, and the calculated total tumor accumulation of  $^{111}\text{In}$ -A7-MMCD at infinite time

after iv injection into SW1116-bearing nude mice and S180-bearing ddY mice. After iv injection into S180-bearing mice the parameters for  $^{14}\text{C}$ -MMCD<sub>an</sub> and  $^{14}\text{C}$ -MMCD<sub>cat</sub>, which both have a molecular weight of 70,000, were calculated from our previous data,<sup>7)</sup> for comparison. In S180-bearing mice, the tissue uptake rate indices in both the liver and spleen and the total body clearance of  $^{111}\text{In}$ -A7-MMCD were one or two orders of magnitude lower than those of  $^{14}\text{C}$ -MMCD<sub>cat</sub>, but only slightly higher than those of  $^{14}\text{C}$ -MMCD<sub>an</sub>, suggesting that A7-MMCD has nearly the same properties as MMCD<sub>an</sub>, which is a negatively charged macromolecule. Pharmacokinetic analysis revealed that there was no large difference in the tissue uptake rate indices for A7-

Table III. AUC, Clearance, and Tissue Uptake Rate for  $^{111}\text{In}$ -A7-MMCD,  $^{14}\text{C}$ -MMCD<sub>an</sub>, and  $^{14}\text{C}$ -MMCD<sub>cat</sub> in Nude Mice Bearing SW1116 or ddY Mice Bearing S180

Compound	AUC (% dose h/ml)	Clearance ( $\mu\text{l}/\text{h}$ )		Tissue uptake rate ( $\mu\text{l}/\text{h}/\text{g}$ )					Total tumor accumulation <sup>a)</sup> (% of dose)
		CL <sub>total</sub>	CL <sub>urine</sub>	Liver	Spleen	Kidney	Muscle	Tumor	
$^{111}\text{In}$ -A7-MMCD <sub>an</sub> (SW 1116)	526	190	—	116	60.4	60.2	2.0	59.8	31.5
$^{111}\text{In}$ -A7-MMCD <sub>an</sub> (S 180)	236	424	2.0	160	73.2	23.8	3.2	23.8	5.6
$^{14}\text{C}$ -MMCD <sub>an</sub> (S 180)	431	232	62.8	58.2	10.3	2.3	1.0	13.6	5.9
$^{14}\text{C}$ -MMCD <sub>cat</sub> (S 180)	15.1	6623	1438	3557	1943	590	7.3	27.1	0.4

a) Calculated by assuming the tumor weight to be 1.0 g.

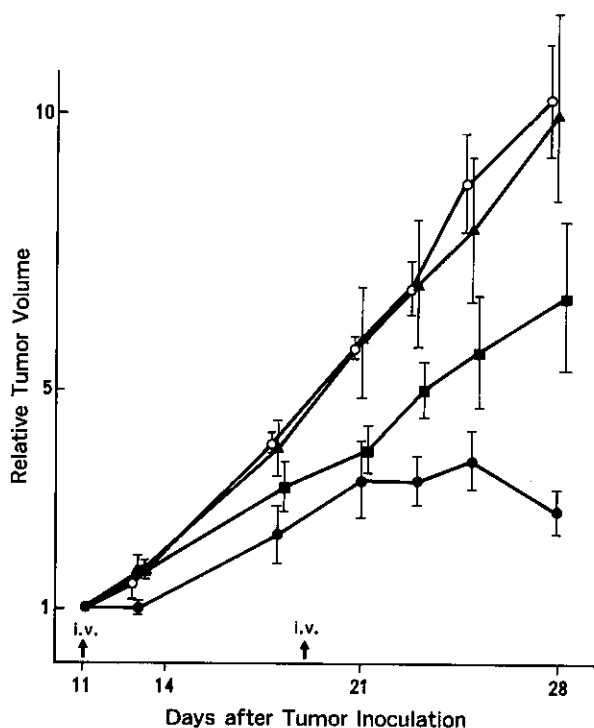


Fig. 2. *In vivo* antitumor activity of A7-MMCD. Groups of four mice were inoculated subcutaneously with SW1116 (day 0). Each group received an iv injection of either PBS (○), 0.5 mg/kg of free MMC (▲), 2.5 mg MMC equivalent/kg of MMCD<sub>an</sub> (■), or 2.5 mg MMC equivalent/kg of A7-MMCD (●) on day 11 and day 19. Results are expressed as the relative tumor volume for each group.

MMCD in the liver and spleen between SW1116- and S180-bearing mice in spite of the differences in total body clearance. On the other hand, the tumor uptake rate index for SW1116 was about 2.5 times greater than that for S180. Furthermore, the total amount of <sup>111</sup>In-A7-MMCD accumulated in SW1116 was calculated to be approximately 5 times greater than the amount in S180, which was almost the same as the amount of <sup>14</sup>C-MMCD<sub>an</sub> in S180. These results indicate that the specific carrier contributes to the accumulation of radioactivity in the target tumor tissue.

**Therapeutic experiment** The *in vivo* antitumor activity of A7-MMCD against the human colon cancer SW1116 transplanted into nude mice was examined. Fig. 2 shows the experimental data obtained, each curve representing the mean tumor volumes of a different group. Since the LD<sub>50</sub> of MMCD<sub>an</sub> was about 5 times higher than that of free MMC, due to the slow release of MMC,<sup>7</sup> the *in vivo* antitumor activities of MMCD<sub>an</sub> and A7-MMCD and that of free MMC were compared at

equitoxic dose levels. In the control group, remarkable tumor growth was observed, and the relative tumor volume 28 days after tumor inoculation was  $9.96 \pm 1.05$  (mean  $\pm$  SE). MMCD<sub>an</sub> had a moderate inhibitory effect on the growth of SW1116 (T/C,  $65 \pm 13\%$ ), whereas free MMC had almost no inhibitory effect on the tumor growth in this concentration range (T/C  $\pm$  SE,  $97 \pm 18\%$ ). The tumor growth of the A7-MMCD-treated group was found to have been significantly suppressed on day 28 (T/C,  $26 \pm 4\%$ ) when compared with that of MMCD<sub>an</sub>-treated mice ( $P < 0.05$  by Student's *t* test) or other groups. No significant weight loss was observed in any group of mice (data not shown).

## DISCUSSION

In preparing an MAb-drug conjugate using a macromolecular intermediate between the MAb and the drug, it must be taken into consideration that the physicochemical properties of the intermediate macromolecule, such as dextran, serum albumin, or synthetic polymers, may alter the *in vivo* behavior of the parent immunoconjugate. There have been numerous evaluations of the *in vivo* distribution of MAb alone<sup>12-14</sup> and more recently several reports have described the distribution of MAb-drug conjugates synthesized by a direct linkage method.<sup>15-18</sup> However, little information is available concerning the *in vivo* distribution characteristics of MAb-drug conjugates synthesized using a macromolecule as an intermediary. In the case of MAb conjugated with plant toxins, such as ricin<sup>19,20</sup> and gelonin,<sup>21</sup> and liposomes containing anticancer agents,<sup>22</sup> the level of accumulation in the tumor tissue after systemic administration markedly decreased compared with unconjugated MAb alone due to increased entrapment by the reticulo-endothelial system. Therefore, the *in vivo* antitumor effects were less successful than would be expected on the basis of the *in vitro* cytotoxic activities. Similarly, the altered disposition characteristics may have lowered the *in vivo* efficacy of the MAb-drug conjugate via an intermediate macromolecule.

In our series of investigations, we have developed a polymeric prodrug of MMC, MMCD<sub>cat</sub>,<sup>23,24</sup> and MMCD<sub>an</sub><sup>9</sup> for passive targeting chemotherapy. The disposition and pharmacokinetics of MMCD were investigated systematically in normal rats after iv<sup>25,26</sup> and intramuscular injection<sup>26,27</sup> and in tumor-bearing mice after iv injection.<sup>7</sup>

Kinetic analysis revealed that MMCD acts as a reservoir of MMC, supplying active MMC to the body.<sup>25,28</sup> A pharmacokinetic study clarified that the physicochemical properties of macromolecules, such as electric charge and molecular weight, mainly determine their biodistribution. For example, MMCD<sub>cat</sub> with a large molecular weight,

such as 500,000, is suitable for local injection because it shows sustained retention at the injection site and enhanced lymphatic delivery, owing to its polycationic nature.<sup>27)</sup> On the contrary, after iv injection, MMCD<sub>cat</sub> is rapidly cleared by the reticuloendothelial system and fails to supply a sufficient amount of the drug to the tumor tissue. Finally, MMCD<sub>an</sub> with a molecular weight of 70,000 is advantageous for tumor targeting since it has a long circulating life with less cellular interaction with the reticuloendothelial system of the liver and spleen, which are the most important organs in determining the *in vivo* systemic disposition of such polymeric prodrugs.<sup>7)</sup> Therefore, we applied these considerations in designing an MAb-drug conjugate and developed a novel immunoconjugate composed of anti-human MAb A7 and MMCD<sub>an</sub> (A7-MMCD) in order to deliver a sufficient amount of MMC efficiently to the targeted tumor tissue with minimal elimination by the reticuloendothelial system. Successful preparations and *in vitro* antitumor activities of A7-MMCD have been reported previously.<sup>6)</sup>

In the present distribution study, <sup>111</sup>In-labeled A7-MMCD showed marked accumulation in the targeted tumor (SW1116), compared to the non-targeted tumor (S180). Radioactivity was also detected in the liver, spleen, and kidney, but the levels of accumulation in these organs were much less than those observed in the case of immunotoxins and immunoliposomes. These results indicated that A7-MMCD, thus synthesized, did achieve site-specific targeting *in vivo*.

Previously, we examined the biodistribution of MAb A7 labeled with <sup>125</sup>I, and 4 days after intraperitoneal injection, a maximal tumor-to-blood ratio of 2.03 and concentration in the tumor tissue of 8.18% dose/g were obtained without significant accumulations in other organs.<sup>29)</sup> In the present study, instead of <sup>125</sup>I, we labeled the conjugate with <sup>111</sup>In. Radioiodination is the most popular method for protein labeling, but radioactivity returns to the blood circulation if the labeled protein is degraded in the organ. On the other hand, by <sup>111</sup>In labeling, the net tissue uptake can be estimated since the radioactivity in the macromolecule is retained for a long period in the tissue owing to uptake into an iron-binding protein<sup>30)</sup> after intracellular degradation. Accordingly, a higher tissue-to-blood ratio can be obtained, but hepatic uptake is also increased by <sup>111</sup>In labeling compared to <sup>125</sup>I labeling. In the present study, significant amounts of radioactivity were also detected in the liver, spleen, and kidney as well as in the tumor tissues of both mice. It is true that this conjugate did accumulate in these organs, but the fact that <sup>111</sup>In was used for the radiolabeling of the conjugate may account for these results.

Pharmacokinetic analysis was performed to assess quantitatively the organ distribution observed in this study. The increased rate of tumor uptake in the targeted

tumor demonstrated that A7-MMCD retains its immunoreactivity *in vivo* and accumulates in the targeted tumor specifically. This high rate of tumor uptake together with the large AUC obtained for the SW1116-bearing nude mice may lead to the high value of total tumor accumulation. Tissue uptake rate indices in the liver and spleen for A7-MMCD in S180-bearing mice were similar to those for MMCD<sub>an</sub> rather than those for MMCD<sub>cat</sub>, which showed that A7-MMCD behaves in almost the same manner as a negatively charged macromolecule *in vivo* against the reticuloendothelial system. These results indicated that our goal of forming an MMC immunoconjugate via an anionic dextran intermediate for specific tumor targeting was close to being achieved, although the actual net electric charge of A7-MMCD was neutral. The slight elevation of the tissue uptake rates in the liver and spleen compared with the rates found using MMCD<sub>an</sub> was probably due to the decreased anionic charge and the increased molecular size of A7-MMCD. A greater anionic charge can be given to MMCD<sub>an</sub> by leaving more unreacted carboxyl groups on the spacer arms of the dextran, at the cost of a reduction in the amount of MMC attached to the dextran. On the other hand, F(ab')<sub>2</sub> fragments of MAb A7 could be successfully obtained by digesting MAb A7 with pepsin as reported previously.<sup>31)</sup> Therefore, A7-MMCD synthesized using an MMCD<sub>an</sub> with a greater anionic charge and a F(ab')<sub>2</sub> fragment instead of whole A7 may exhibit improved tumor localization with lower rates of tissue uptake in the liver and spleen.

Since the lysyl residues of the antibody molecule were labeled with <sup>111</sup>In through DTPA, the radioactivity detected might not necessarily represent the *in vivo* behavior of the conjugate. The disulfide bond between the antibody and the dextran might be broken in the body as observed in the case of ricin conjugated with antibody employing SPDP.<sup>32)</sup> But, it has recently been revealed that the stability of the disulfide bond depends on the degree of folding and subsequent protection of the disulfide linkages between macromolecules.<sup>33)</sup> In the case of A7-MMCD, since a greater *in vivo* antitumor activity was observed in the therapeutic experiment, it was thought that the disulfide bond in A7-MMCD is fairly stable in the circulation and that the radioactivity represents the tissue distribution of MMCD in the conjugated form. An *in vivo* stability test and a biodistribution study which will label the dextran component of A7-MMCD will be the next step in our study.

In the preliminary therapeutic experiment, A7-MMCD significantly suppressed tumor growth in comparison with free MMC and MMCD<sub>an</sub>. The remarkable ability of A7-MMCD to accumulate in the tumor observed in the distribution study may contribute to the observed growth-inhibitory effect on human colon cancer

implanted subcutaneously. Since A7-MMCD, a prodrug of MMC, liberates active MMC with a half-life of about 30 h in the body, not enzymatically but by chemical hydrolysis,<sup>25)</sup> the *in vivo* antitumor activity of A7-MMCD was presumably brought about mainly by free MMC dissociated from the conjugate bound on the cell surface. Therefore, endocytic internalization, which is an essential process for some immunoconjugates that exhibit their selective cytotoxicity through degradation by lysosomal enzymes,<sup>34)</sup> may be disadvantageous for A7-MMCD and may greatly affect the cytotoxicity of A7-MMCD. In this way, besides internalization, various factors, such as mode of action, MMC release rate, and tumor size, may play important roles in determining the efficacy of A7-MMCD. Optimization of the treatment

schedule is to be investigated by further detailed experiments.

In conclusion, our novel immunoconjugate, A7-MMCD, which was prepared via an anionic dextran intermediate for the purpose of keeping the non-specific uptake by the reticuloendothelial system to a minimum, achieved site-specific targeting in the body, leading to a greater *in vivo* antitumor activity. These results suggest that to obtain an MAbs-drug conjugate via an intermediary which is efficacious *in vivo*, it is of great importance to select the appropriate intermediate carrier, i.e. one that has advantageous physicochemical properties for systemic tumor targeting.

(Received August 29, 1990/Accepted November 6, 1990)

## REFERENCES

- 1) Ghose, T. The design of cytotoxic-agent-antibody conjugates. *CRC Crit. Rev. Ther. Drug Carrier Syst.*, **3**, 263-359 (1987).
- 2) Takahashi, T., Yamaguchi, T., Kitamura, K., Suzuyama, H., Honda, M., Yokota, T., Kotanagi, H., Takahashi, M. and Hashimoto, Y. Clinical application of monoclonal antibody-drug conjugates for immunotargeting chemotherapy of colorectal carcinoma. *Cancer*, **61**, 881-888 (1988).
- 3) Arnon, R., and Sela, M. *In vitro* and *in vivo* efficacy of conjugates of daunomycin with anti-tumor antibodies. *Immunol. Rev.*, **62**, 5-27 (1982).
- 4) Garnett, M. C., Embleton, M. J., Jacob, E. and Baldwin, R. W. Preparation and properties of a drug-carrier-antibody conjugate showing selective antibody-directed cytotoxicity *in vitro*. *Int. J. Cancer*, **31**, 661-670 (1983).
- 5) Tsukada, Y., Kato, Y., Umamoto, N., Takeda, Y., Hara, T. and Hirai, H. An anti-alpha-fetoprotein antibody-daunomycin conjugate with a novel poly-L-glutamic acid derivative as intermediate carrier. *J. Natl. Cancer Inst.*, **13**, 721-729 (1984).
- 6) Noguchi, A., Takahashi, T., Yamaguchi, T., Kitamura, K., Yokota, T., Takakura, Y., Hashida, M. and Sezaki, H. Preparation and properties of immunoconjugate composed of anti-human colon cancer monoclonal antibody and mitomycin C-dextran conjugate. *Bioconjugate Chem.* (1991), in press.
- 7) Takakura, Y., Takagi, A., Hashida, M. and Sezaki, H. Disposition and tumor localization of mitomycin C-dextran conjugates in mice. *Pharm. Res.*, **4**, 293-300 (1987).
- 8) Kotanagi, H., Takahashi, T., Masuko, T., Hashimoto, Y. and Koyama, K. A monoclonal antibody against human colon cancers. *Tohoku J. Exp. Med.*, **148**, 353-360 (1986).
- 9) Takakura, Y., Kitajima, M., Matsumoto, S., Hashida, M. and Sezaki, H. Development of a novel polymeric prodrug of mitomycin C, mitomycin C-dextran conjugate with anionic charge. I. Physicochemical characteristics and *in vivo* antitumor activities. *Int. J. Pharm.*, **37**, 135-143 (1987).
- 10) Hnatowich, D. J., Childs, R. L., Lanteigne, D. and Najafi, A. The preparation of DTPA-coupled antibodies radiolabeled with metallic radionuclides: an improved method. *J. Immun. Methods*, **65**, 147-157 (1983).
- 11) Yamaoka, K. and Nakagawa, T. A nonlinear least-squares program based on differential equations, MULTI-(RUNGE), for microcomputers. *J. Pharmacobio-Dyn.*, **6**, 595-606 (1983).
- 12) Herlyn, D., Powe, J., Alavi, A., Mattis, J. A., Herlyn, M., Ernst, C., Vaum, R. and Koprowski, H. Radioimmuno-detection of human tumor xenografts by monoclonal antibodies. *Cancer Res.*, **43**, 2731-2735 (1983).
- 13) Colcher, D., Keenan, A. M., Larson, S. M. and Schlom, J. Prolonged binding of a radiolabeled monoclonal antibody (B72.3) used for the *in situ* radioimmunodetection of human colon carcinoma xenografts. *Cancer Res.*, **44**, 5744-5751 (1984).
- 14) Zalcborg, J. R., Thompson, C. H., Lichtenstein, M., Andrews, J. and McKenzie, I. F. C. Localization of human colorectal tumor xenografts in the nude mouse with the use of radiolabeled monoclonal antibody. *J. Natl. Cancer Inst.*, **71**, 801-808 (1983).
- 15) Ballantyne, K. C., Perkins, A. C., Pimm, M. V., Garnett, M. C., Clegg, J. N., Armitage, N. C., Baldwin, R. W. and Hardcastle, J. D. Biodistribution of a monoclonal antibody-methotrexate conjugate (791/36-MTX) in patients with colorectal cancer. *Int. J. Cancer*, **2** (Suppl.), 103-108 (1988).
- 16) Pimm, M. V., Paul, M. A., Ogumuyiwa, Y. and Baldwin, R. W. Biodistribution and tumor localization of a daunomycin-monoclonal antibody conjugate in nude mice with human tumor xenografts. *Cancer Immunol. Immunother.*

- 27, 267-271 (1988).
- 17) Rowland, G. F., Simmonds, R. G., Gore, V. A., Marsden, C. H. and Smith, W. Drug localization and growth inhibition studies of vindesine-mono-clonal anti-CEA conjugates in a human tumor xenograft. *Cancer Immunol. Immunother.*, **21**, 183-187 (1986).
  - 18) Spearman, M. E., Goodwin, R. M. and Kau, D. Disposition of the monoclonal antibody-vinca alkaloid conjugate, KS1/4-DAVLB(LY256787), in Fischer 344 rats and rhesus monkeys. *Drug Metab. Disp.*, **15**, 640-647 (1987).
  - 19) Bourrie, B. J. P., Casellas, P., Blythman, H. E. and Jansen, F. K. Study of the plasma clearance of antibody ricin-A-chain immunotoxins. Evidence for specific recognition sites on the A chain that mediate rapid clearance of the immunotoxin. *Eur. J. Biochem.*, **155**, 1-10 (1986).
  - 20) Worrell, N. R., Cumber, A. J., Parnell, G. D., Ross, W. C. and Forrester, J. A. Fate of an antibody-ricin A chain conjugate administered to normal rats. *Biochem. Pharmacol.*, **35**, 417-423 (1986).
  - 21) Scott, C. E., Jr., Lambert, J. M., Goldmacher, V. S., Blattler, W. A., Sobel, R., Schlossman, S. F. and Benacerraf, B. The pharmacokinetics and toxicity of murine monoclonal antibodies and of gelonin conjugates of these antibodies. *Int. J. Immunopharm.*, **9**, 211-225 (1987).
  - 22) Dobs, R. J., Heath, T. D. and Papahadjopoulos, D. Targeting of anti-thy 1.1 monoclonal antibody conjugated liposomes in Thy 1.1 mice after intravenous administration. *Biochim. Biophys. Acta*, **901**, 183-190 (1987).
  - 23) Sezaki, H. and Hashida, M. Macromolecular-drug conjugates in targeted cancer chemotherapy. *CRC Crit. Rev. Ther. Drug Carrier Syst.*, **1**, 1-38 (1984).
  - 24) Kojima, T., Hashida, M., Muranishi, S. and Sezaki, H. Mitomycin C-dextran conjugate: a novel high molecular weight prodrug of mitomycin C. *J. Pharm. Pharmacol.*, **32**, 30-34 (1980).
  - 25) Hashida, M., Kato, A., Takakura, Y. and Sezaki, H. Disposition and pharmacokinetics of a polymeric prodrug of mitomycin C, mitomycin C-dextran conjugate, in the rat. *Drug Metab. Disp.*, **12**, 492-499 (1984).
  - 26) Takakura, Y., Atsumi, R., Hashida, M. and Sezaki, H. Development of a novel polymeric prodrug of mitomycin C, mitomycin C-dextran conjugate with anionic charge. II. Disposition and pharmacokinetics following intravenous and intramuscular administration. *Int. J. Pharm.*, **37**, 145-154 (1987).
  - 27) Takakura, Y., Matsumoto, S., Hashida, M. and Sezaki, H. Enhanced lymphatic delivery of mitomycin C conjugated with dextran. *Cancer Res.*, **44**, 2505-2510 (1984).
  - 28) Hashida, M., Takakura, Y., Matsumoto, S., Sasaki, H., Kato, A., Kojima, T., Muranishi, S. and Sezaki, H. Regeneration characteristics of mitomycin C-dextran conjugate in relation to its activity. *Chem. Pharm. Bull.*, **31**, 2055-2363 (1983).
  - 29) Takahashi, M. *In vivo* localization of monoclonal antibody A-7 in human colon cancer inoculated into nude mice. *Akita J. Med.*, **12**, 415-468 (1985) (in Japanese).
  - 30) Brown, B. A., Comeau, R. D., Jones, P. L., Liberatore, F. A., Neacy, W. P., Sands, H. and Gallagher, B. M. Pharmacokinetics of the monoclonal antibody B72.3 and its fragments labeled with either <sup>125</sup>I or <sup>111</sup>In. *Cancer Res.*, **47**, 1149-1154 (1987).
  - 31) Kitamura, K., Takahashi, T., Yamaguchi, T., Kitai, S., Amagai, T. and Imanishi, J. Monoclonal antibody A7 tumor localization enhancement by its F(ab')<sub>2</sub> fragments to colon carcinoma xenografts in nude mice. *Jpn. J. Oncol.*, **20**, 139-144 (1990).
  - 32) Thorpe, P. E. and Ross, W. C. J. The preparation and cytotoxic properties of antibody-toxin conjugates. *Immunol. Rev.*, **62**, 119-158 (1982).
  - 33) Sivam, G., Pearson, J. W., Oldham, R. K., Sadoff, J. C. and Morgan, A. C., Jr. Immunotoxins to a human melanoma-associated antigen: comparison of gelonin with ricin and other A chain conjugates. *Cancer Res.*, **47**, 3169-3173 (1987).
  - 34) Shen, W. C., Ballou, B., Ryser, H. J-P. and Hakala, T. R. Targeting, internalization, and cytotoxicity of methotrexate-mono-clonal anti-stage-specific embryonic antigen-1 antibody conjugates in cultured F-9 teratocarcinoma cells. *Cancer Res.*, **46**, 3912-3916 (1986).